SUPPLEMENTAL MATERIAL

Kesavardhana et al., https://doi.org/10.1084/jem.20170550

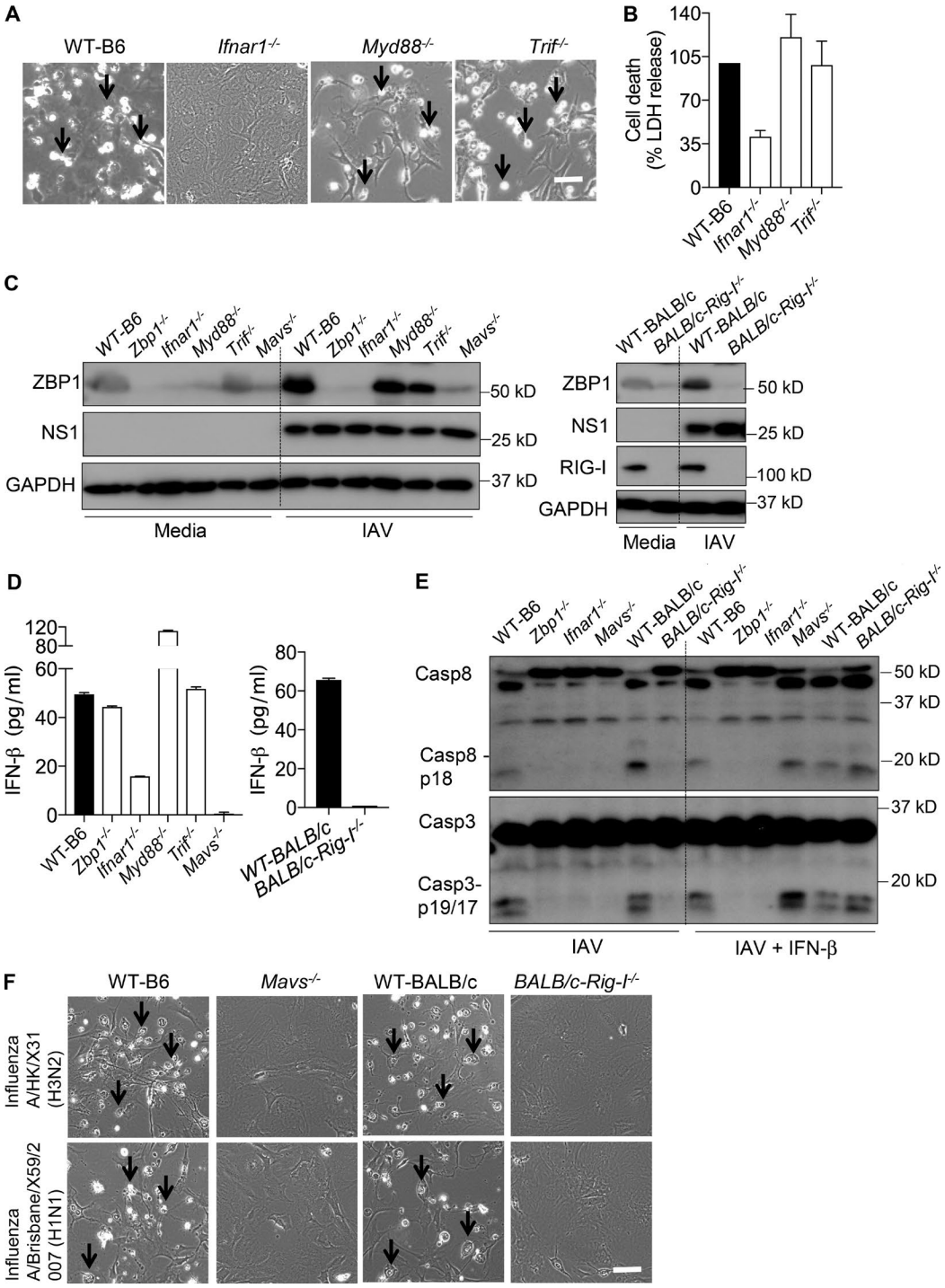


Figure S1. **Role of IFNAR, TLR, and RIG-I–MAVS signaling pathways for ZBP1-mediated cell death in response to IAV.** (A and B) The TLR adaptor proteins MyD88 and TRIF are dispensable for IAV-induced cell death. (A) Microscopic analysis of cell death in unprimed primary fibroblasts infected with IAV (MOI, 10) after 20 h of infection ($n = 4$). Arrows indicate dead cells after IAV infection. Bar, 100 µm. (B) Quantification of cell death by LDH release in unprimed primary fibroblasts infected with IAV (MOI, 10) after 20 h. LDH release was normalized to IAV-infected WT cells ($n = 3$). (C) Immunoblot analysis of ZBP1, RIG-I, NS1, and GAPDH (loading control) in fibroblasts infected with IAV. The expression levels of all proteins are compared with the expression pattern in uninfected fibroblasts ($n = 3$). (D) Levels of IFN-β in cell culture supernatants 12 h after infection with IAV. (E) Immunoblot analysis of the pro- and cleaved forms of caspase-8 and caspase-3 in fibroblasts 20 h after infection with IAV and IAV in combination with 100 U/ml IFN-β ($n = 3$). (F) Microscopic analysis of cell death in fibroblasts infected with mouse adapted influenza A/X31(H3N2) and influenza A/Brisbane/59/2007(H1N1) after 20 h ($n = 3$). Arrows indicate dead cells after IAV infection. Bar, 100 µm. Data are representative of three independent experiments (mean ± SEM).

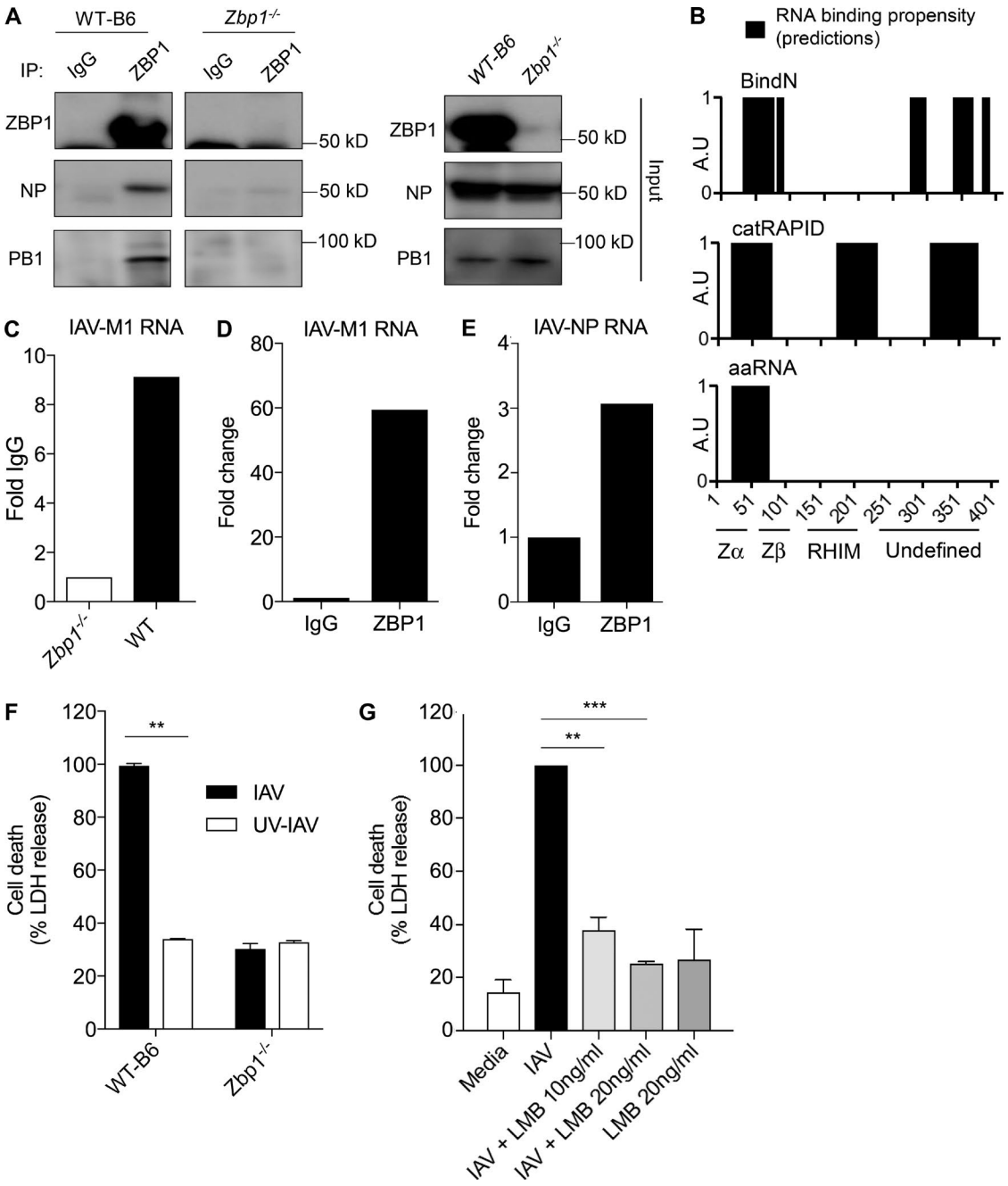


Figure S2. **ZBP1 interacts with IAV proteins NP, PB1, and IAV RNA in IAV-infected cells.** (A) Immunoprecipitation (IP) of endogenous ZBP1 from lysates of WT or *Zbp1*$^{-/-}$ fibroblasts infected with IAV for 12 h and immunoblotted for ZBP1, PB1, and NP ($n$ = 3). (B) RNA-binding propensity of ZBP1 assessed using three different protein-RNA–binding prediction analytical tools: BindN, catRAPID, and aaRNA. A.U, arbitrary unit. x axis, amino acid residue number and domains of the mouse ZBP1 protein. (C–E) Real-time quantitative RT-PCR for IAV RNA bound to ZBP1 immunoprecipitated from WT and *Zbp1*$^{-/-}$ fibroblasts (C) and WT-fibroblasts (D and E) after 12-h IAV infection ($n$ = 4). (F and G) Replication of IAV and nuclear export of IAV RNP complexes are essential for IAV-induced cell death. (F) Quantitation of cell death by LDH release in primary fibroblasts infected with IAV or UV-irradiated IAV (UV-IAV) after 20 h ($n$ = 3). **, P < 0.006 (two-tailed $t$ test). (G) Quantitation of cell death by LDH release in fibroblasts infected with IAV or IAV in combination with LMB after 20 h. **, P = 0.002; ***, P = 0.0009 (one-way ANOVA). Data are representative of three independent experiments (mean ± SEM).

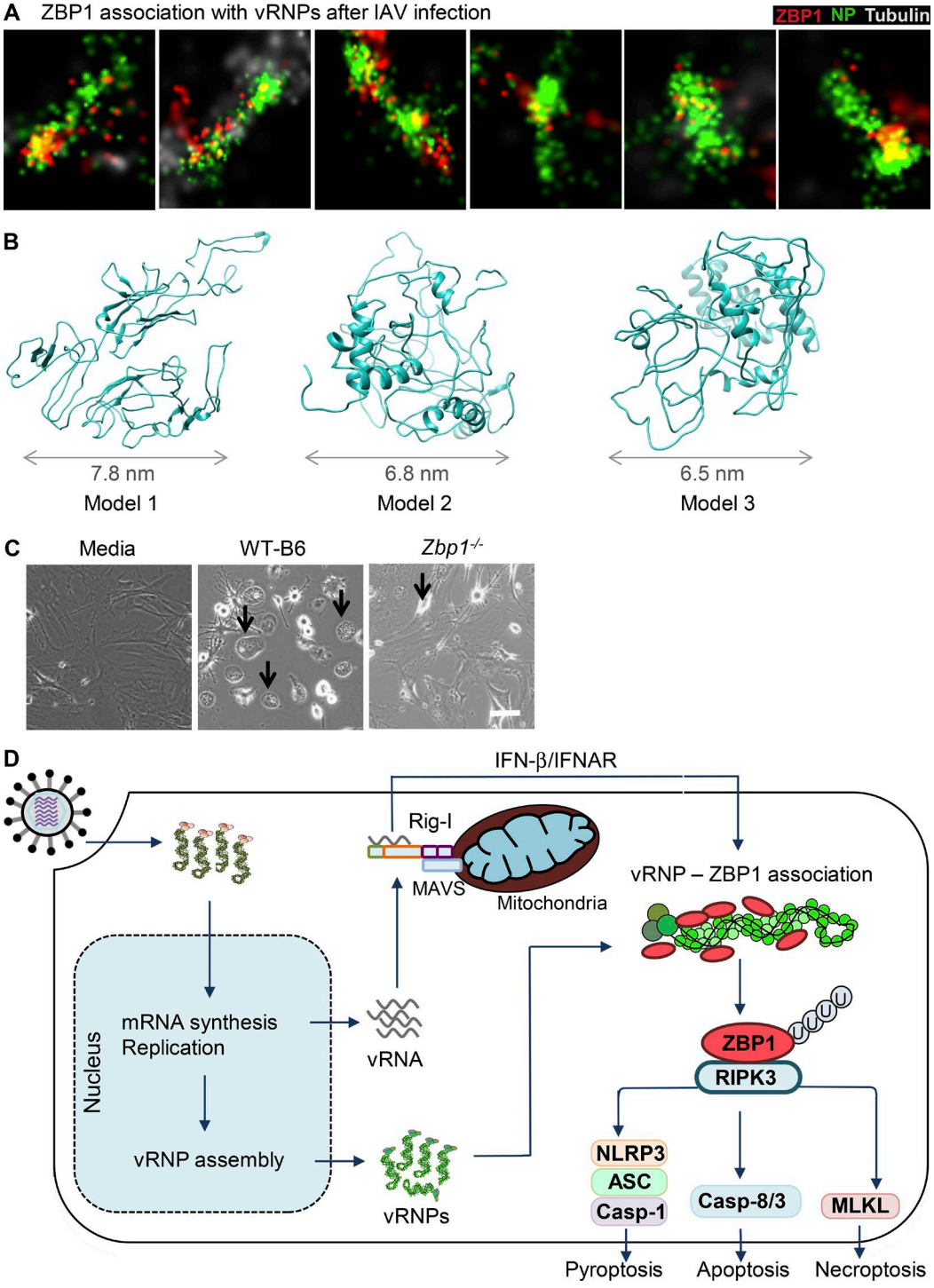


Figure S3. **Recognition of vRNPs by ZBP1 during viral infections.** (A) Primary fibroblasts were infected with IAV and subjected to three-dimensional STORM 8 h after infection. Multiple zoomed-in images showing NP stained vRNPs (green) in close proximity to ZBP1 (red). (B) Cartoon representation of top predicted models of the full-length ZBP1 structure. (C) ZBP1 regulates MCMV-induced cell death. Microscopic analysis of cell death in fibroblasts infected with MCMV virus (MOI 15). Images were collected 2 h after MCMV infection ($n = 2$). Arrows indicate dead cells after IAV infection. Bar, 100 µm. (D) Model representing IAV-induced ZBP1 activation to trigger programmed cell death. RIG-I senses IAV-RNA and associates with MAVS at the outer mitochondrial membrane. RIG-I–MAVS signaling up-regulates IFN-β–dependent ZBP1 expression and activation. IAV infection also induces ZBP1 ubiquitination. ZBP1 recognizes vRNP complexes generated after IAV replication. Activated ZBP1, in association with RIPK3, triggers programmed cell death pathways. ASC, apoptosis-associated speck-like protein containing a caspase-activation and recruitment domain; MLKL, mixed lineage kinase domain–like pseudokinase.